

## Magnetic order and lattice anomalies in the $J_1$ - $J_2$ model system $\text{VOMoO}_4$

A. Bombardi,<sup>1</sup> L. C. Chapon,<sup>2</sup> I. Margiolaki,<sup>3</sup> C. Mazzoli,<sup>3</sup> S. Gonthier,<sup>4</sup> F. Duc,<sup>4</sup> and P. G. Radaelli<sup>2,5</sup>

<sup>1</sup>*Diamond Light Source Ltd., Rutherford Appleton Laboratory, Chilton-Didcot, OX11 0QX, Oxfordshire, United Kingdom*

<sup>2</sup>*ISIS, CCLRC Rutherford Appleton Laboratory, Chilton-Didcot, OX11 0QX, Oxfordshire, United Kingdom*

<sup>3</sup>*European Synchrotron Radiation Facility, BP 220, 38043 Grenoble Cedex 9, France*

<sup>4</sup>*Centre d'Elaboration des Matériaux et d'Etudes Structurales, CNRS, 31055 Toulouse Cedex, France*

<sup>5</sup>*Department of Physics and Astronomy, University College London, London WC1E 6BT, United Kingdom*

(Received 11 February 2005; published 14 June 2005)

High-resolution x-ray and neutron powder-diffraction measurements were performed on polycrystalline  $\text{VOMoO}_4$ . Below  $\approx 40$  K the system orders in a simple Néel antiferromagnetic state (propagation vector  $\vec{k} = 0$ ), indicating a dominant role of the nearest-neighbor interactions. The order is three dimensional but the reduced saturated magnetic moment  $m$  of  $0.41(1) \mu_B/\text{V}^{4+}$  at 2 K indicates strongly two-dimensional character and enhanced quantum fluctuations. On cooling, there is no evidence of a reduction of the crystal symmetry. However, neutron diffraction indicates an anomalous evolution of the lattice parameters, which can be related to the onset of magnetic correlations.

DOI: 10.1103/PhysRevB.71.220406

PACS number(s): 75.25.+z, 61.12.-q

Frustrated magnets based on transition metals have become subjects of many theoretical and experimental studies in the past years:<sup>1,2</sup> a variety of exotic quantum effects are expected when competitive interactions lead a system into a frustrated state, where it is impossible to satisfy all the pair interactions simultaneously. One of the most studied model systems is the spin-1/2 Heisenberg antiferromagnet on a square lattice with competing nearest- ( $J_1$ ) and next-nearest- ( $J_2$ ) neighbor antiferromagnetic interactions. In two dimensions, the zero-point quantum fluctuations (enhanced by a low spin value), combined with the frustration, are strong enough to destroy the long range ordering in the system even at zero temperature. The two limiting cases of this model are relatively simple and well understood: when  $J_1 \gg J_2$ , the system orders into a simple Néel state, whereas when  $J_1 \ll J_2$  the problem can be treated in terms of two decoupled interpenetrating Néel lattices. In the mean-field limit, all the relative orientations of these two sublattices have the same energy, but the order-by-disorder mechanism<sup>3</sup> lowers the energy of the collinear states. The intermediate situation is still a matter of debate; in particular, different predictions exist concerning the magnetic and nonmagnetic ground states in the vicinity of the fully frustrated point ( $J_1 \approx 2 \times J_2$ ) (Ref. 4).

Recently, several new vanadium-based compounds have provided experimental realizations of the  $J_1$ - $J_2$  model, and are currently receiving significant attention by the scientific community. The first widely studied prototype of this family was  $\text{Li}_2\text{VOSiO}_4$  (Ref. 5). At low temperature, this material was found to order in the collinear magnetic state.<sup>6-8</sup> The staggered magnetization from neutron scattering was found to be  $0.63 \mu_B$ , in excellent agreement with  $J_2/J_1 \approx 12$ , as obtained from band-structure calculations and bulk properties measurements.<sup>9</sup>

Another window into this phase diagram is provided by the closely related system  $\text{VOMoO}_4$  (Ref. 10). Initially,  $\text{VOMoO}_4$  was considered as a weak one-dimensional antiferromagnet.<sup>11-13</sup> However, recent band-structure calculations by Carretta *et al.*<sup>14</sup> have shown that this system is

essentially two dimensional (2D), with extremely weak interplanar coupling. The crystal structure of  $\text{VOMoO}_4$ , shown in Fig. 1, presents many similarities with  $\text{Li}_2\text{VOSiO}_4$ .  $\text{VOMoO}_4$  crystallizes in the tetragonal space group  $P4/n$  (No. 85), with two formula units per cell, the spin-1/2  $\text{V}^{4+}$  ions forming a network of  $\text{VO}_5$  square pyramids, sharing corners with  $\text{MoO}_4$  tetrahedra. The main differences with respect to  $\text{Li}_2\text{VOSiO}_4$  (space group  $P4/nmm$ ) are the absence of Li to separate the layers, the fact that the apical oxygens of the  $\text{VO}_5$  pyramids point away rather than toward the interior of the  $\text{MoVO}_5$  layers and the rotations of both  $\text{VO}_5$  and  $\text{MoO}_4$  polyhedra, resulting in the loss of the mirror planes.

Carretta *et al.*<sup>14</sup> measured the magnetic susceptibility and the electron-paramagnetic-resonance signal of  $\text{VOMoO}_4$ ,

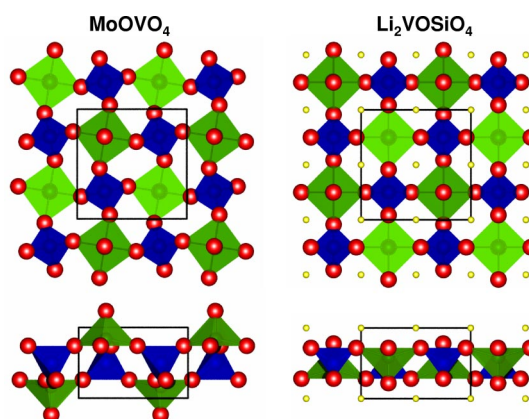


FIG. 1. (Color online) Comparison between the crystallographic structure of  $\text{VOMoO}_4$  (left) and  $\text{Li}_2\text{VOSiO}_4$  (right). Two projections are shown along  $[001]$  (top) and  $[100]$  (bottom) for each crystal. The small circles are the Li ion. The  $\text{Mo(Si)O}_4$  tetrahedra are drawn in dark gray, whereas the  $\text{V}_4$  pyramids are drawn in light gray. Due to the reversal of the pyramids along  $z$  in the  $[001]$  projections half of the V are hidden by the apical oxygen  $[\text{O}(1)]$ . The unit cell is indicated by solid lines.

and showed that the magnetic properties of  $\text{Li}_2\text{VOSiO}_4$  and  $\text{VOMoO}_4$  are quite similar, once normalized to their ordering temperatures ( $T_N=2.8$  and 42 K, respectively). This was taken as a strong indication that the two systems are in the same region of the phase diagram ( $J_1 \approx J_2$ ). Intriguingly,  $^{95}\text{Mo}$  nuclear magnetic resonance (NMR) evidenced a local lattice distortion occurring at about 100 K, which was explained with the necessity to remove the frustration of the nearest-neighbor (NN) interactions, through the so-called spin Jahn-Teller mechanism.<sup>15</sup> The modulation of the NN interaction would occur through a small charge transfer from the V to the Mo site. Both magnetization and NMR measurement<sup>14</sup> clearly indicate a transition to a magnetic ground state occurring at about 42 K. Although the exact nature of this ground state could not be determined from these bulk measurements, Carretta predicts a collinear ordering, as expected for  $J_1 \approx J_2$ . The consistency of this picture is challenged by band-structure calculations carried out by the same authors,<sup>14</sup> which would place  $\text{VOMoO}_4$  on the *other* side of the phase diagram ( $J_1 > J_2$ , with  $J_1/J_2 \approx 5-10$ ). This discrepancy is attributed to an inadequate modeling of the electron-electron interactions in the band-structure calculation. In this paper, we present high-resolution x-ray and neutron powder-diffraction measurements on polycrystalline samples of  $\text{VOMoO}_4$ . Contrary to the expectations, but consistent with Carretta *et al.*'s band-structure calculations,  $\text{VOMoO}_4$  orders into a simple Néel state, implying  $J_1 \gg J_2$ . This is further confirmed by the refined low-temperature value of the magnetic moment ( $0.41\mu_B$ ), which is consistent with  $J_2 \approx 0.2 \times J_1$ . In agreement with Carretta *et al.*'s findings, we found clear evidence in the lattice parameters of a structural anomaly on cooling below 150 K, and other structural changes are consistent with a continuous transfer of charge to the Mo. However, these effects can no longer be attributed to the spin Jahn-Teller mechanism. Rather, we suggest that the structural distortion reduces the next-nearest-neighbor (NNN) interaction, pushing the system further toward the unfrustrated limit.

The synthesis of the  $\text{VOMoO}_4$  samples is described in Ref. 14. High-resolution synchrotron x-ray powder-diffraction data were collected at 20 and 80 K with a wavelength  $\lambda=0.499\,530(8)$  Å, using the high-resolution powder-diffraction beamline ID31 at the ESRF, Grenoble. The 80-K data were well refined in the space group  $P4/n$ , with  $R_{F2} \approx 0.088$ . No additional Bragg peaks appeared on cooling, and the refinement of the low-temperature (20-K) diffraction pattern in the same space group  $P4/n$  gave a very similar agreement factor ( $R_{F2} \approx 0.103$ ). A close inspection of the data shows very weak additional peaks but these features are present at both temperature (either seen as an asymmetric profile or weak shoulders). Therefore, they seem to be related to an unknown impurity phase. Neutron powder-diffraction data were collected using the general materials diffractometer GEM at the ISIS pulsed neutron source. Data in the temperature range 1.8-250 K were collected on warming, using a helium cryostat. A second set of data with finer temperature spacing was collected on warming between 7 and 50 K, using a closed-cycle refrigerator (displex), and was found to be fully consistent with the first set in the

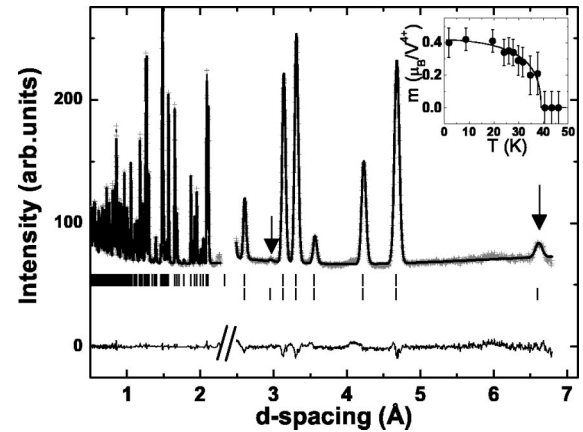


FIG. 2. Neutron powder-diffraction pattern collected at 1.8 K; two of the GEMS detector banks are shown; the data collected in the two banks are shifted and multiplied by two different constants for the sake of lisibility. The arrows indicate the positions of the observed magnetic peaks, the vertical lines are the position of the peaks calculated by Rietveld refinement for the structural (upper) and the magnetic (lower) phases. The difference between the observed and the calculated profile is also shown on the bottom. In the temperature dependence of the magnetic moment, shown in the inset, the solid line is a guide for the eye.

region of overlap. A diffraction pattern collected at 1.8 K in the neutron experiment is shown in Fig. 2. Rietveld analysis<sup>16</sup> of the diffraction pattern was carried out using the FullProf Suite.<sup>17</sup> The  $\text{VOMoO}_4$  nuclear structure as determined from the neutron data is fully consistent with the x-ray results. In particular, within the experimental resolution,  $\text{VOMoO}_4$  appears to be metrically tetragonal in the temperature range  $1.8 \leq T \leq 250$  K, with no evidence of symmetry lowering transitions.

Two resolution-limited extra peaks indicated by the arrows in Fig. 2, which are forbidden in the space group  $P4/n$ , appear below 40 K. This temperature is close to the Néel temperature ( $T_N=42$  K) as determined by magnetic susceptibility and other local probes, indicating that the new peaks are magnetic. The appearance of the (1,0,0) magnetic peak at 6.7 Å immediately allows one to identify  $\vec{k}=0$  as the propagation vector of the magnetic structure. This also rules out the same collinear order of  $\text{Li}_2\text{VOSiO}_4$ , which has a propagation vector  $\vec{k}=(1/2,1/2,0)$ . A propagation vector  $\vec{k}=0$  would be compatible with a FM structure but the presence of peaks not allowed by the crystal symmetry also excludes this possibility. It should be noticed that Shiozaki<sup>11</sup> suggested that a weak FM component might be present in this compound at low  $T$ . The detection limit for such a component with neutron diffraction is  $\approx 0.1\mu_B$ , however such a component would lead to a canted magnetic structure which is not symmetry allowed in the Landau framework of continuous transitions. We used the program BASIREPS (Ref. 18) to search systematically the irreducible representations (IR) of the propagation vector group ( $P4/n$ ) and the corresponding basis functions for the V site. The magnetic representation is reduced into six one-dimensional (1D) IRs:  $\Gamma_1+\Gamma_2+(\Gamma_3+\Gamma_7)+(\Gamma_4+\Gamma_8)$  following Kovalev's convention,<sup>19</sup> where ( $\Gamma_3=\Gamma_7^*$  and  $\Gamma_4=\Gamma_8^*$ ). Therefore, assuming a second-order

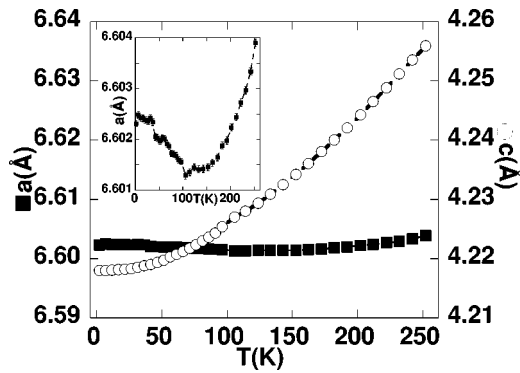


FIG. 3. Change of the tetragonal lattice parameters  $a$  and  $c$  with  $T$  plotted on the same scale. In the inset, zoom on the temperature evolution of the  $a$  lattice parameter.

transition, a maximum of one parameter suffices to determine the magnetic structure. Excluding FM ordering and taking symmetry into account, there are only two possible magnetic structures, both corresponding to simple Néel ordering, with collinear magnetic moments pointing either along the  $c$  axis or in the  $ab$  plane. This is clearly different from the case of  $\text{Li}_2\text{VOSiO}_4$ , where symmetry allows both collinear and noncollinear ordering.<sup>8</sup> It is noteworthy that Shubnikov symmetry analysis<sup>20</sup> would only allow moments along the  $c$  axis (magnetic space group  $P4/n'$  for the AFM structure and  $P4/n$  for the FM structure, since only  $\Gamma_1$  and  $\Gamma_2$  are real representations.

Due to the small number of observed magnetic peaks, the two possible AFM structures are essentially indistinguishable, and gave the same agreement factor and saturated magnetic moment  $m=0.41(1)\mu_B/\text{V}^{4+}$ . The temperature dependence of the magnetic moment is shown in the inset of Fig. 2. It is clear that the moment is saturated at low temperature, but it is impossible to extract a reliable order parameter from these data. The sharpness of the magnetic reflections clearly indicates three-dimensional (3D) ordering, but this is not uncommon in 2D systems with a weak coupling in the third dimension, and was also observed in  $\text{Li}_2\text{VOSiO}_4$ . A more reliable indication of the dimensionality of the system is given by the value of the magnetic moment ( $0.41\mu_B/\text{V}^{4+}$ ). Assuming  $S=1/2$  and no orbital contribution, this value is too low for a 3D-ordered system ( $1\mu_B/\text{V}^{4+}$ ), but it is only slightly lower than what is expected for a 2D nonfrustrated system ( $0.6\mu_B/\text{V}^{4+}$  for  $J_2=0$ ). Theoretical models predict that the moment will smoothly decrease as a function of  $J_2/J_1$  towards the nonmagnetic ground state. In particular, our measured magnetic moment ( $0.41\mu_B$ ) would indicate  $J_2 \approx 0.2 \cdot J_1$  (Refs. 21 and 22), in excellent agreement with Carretta *et al.*'s band-structure calculations.

As already mentioned, there is no evidence of a structural phase transition, even in the high-resolution x-ray synchrotron data. However, we were able to follow the evolution of the crystal structure in detail, and relate it to the anomalies observed by Carretta in the  $^{95}\text{Mo}$  NMR. The temperature dependence of the lattice parameters is shown in Fig. 3. As expected for 2D systems, the  $c$  parameter shows much greater thermal expansion (0.9% from 2 to 250 K) than the in-plane parameter. Both  $a$  and  $c$  display anomalies above

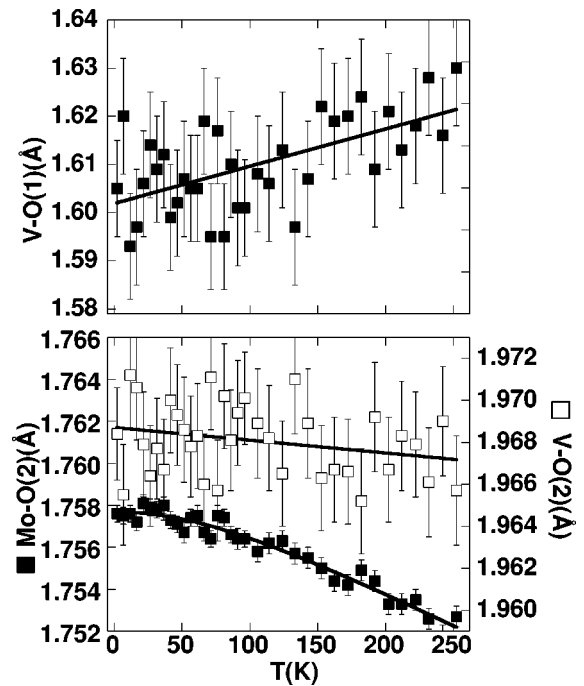


FIG. 4. (Top) temperature change of the V–O(1) distance, the data are noisy due to the neutron difficulty to access the V position (see main text). (Bottom) temperature change of the Mo–O(2) and V–O(2) distance.

100 K, a clear minimum for  $a$  and a small change of slope for  $c$ . These anomalies are also reflected in the unit-cell volume  $V$ : an attempt to fit its temperature dependence using the Debye model in the first-order Grüneisen approximation systematically underestimates the low-temperature values and overestimates all the data above 120 K.

A closer inspection (see inset of Fig. 3) demonstrates that the anomalous trend of the  $a$  parameter starts at about 170 K, with the lattice parameter going through a broad minimum at  $T_{\min} \approx 150$  K and expanding on cooling down to the lowest measured temperature. A small jump can be observed near the magnetic transition (40 K), although it is unclear whether this is statistically significant. Carretta attributes the observed NMR anomaly to the transfer of charge between  $\text{V}^{4+}$  and  $\text{Mo}^{6+}$ , so that the oxidation state of the latter would be reduced. We have looked for the signature of this charge transfer in the internal structural parameters (bond lengths and angles), which were determined at all temperatures by Rietveld refinements based on our neutron data. A selection of the bond lengths is shown in Fig. 4. Due to the small coherent scattering length of V for neutrons, all the parameters containing the V fractional coordinate  $z$  have rather large error bars. Nevertheless, it is clear that the VO(1) bond is the major one responsible for the thermal expansion along the  $c$  axis. Both in-plane VO(2) and MoO(2) distances increase on cooling, but the effect on the MoO(2) is much more pronounced. To accommodate the negative thermal expansion of the MoO(2) and VO(2) bonds, having their largest projection in the  $ab$  plane, the system *decreases* the rotation of the polyhedra, so that the Mo–O(2)–V bond angle *increases* from  $\approx 150.3^\circ$  at 1.8 K to  $\approx 150.7^\circ$  at 250 K.



The expansion of the Mo–O(2) bond length on cooling may be interpreted as due to an increasing population of the Mo  $d_{xy}$  orbitals, and is therefore consistent with a transfer of charge from  $V^{4+}$  to  $Mo^{6+}$ . However, this change occurs *continuously* on cooling from room temperature, and cannot be attributed to the onset of short-range magnetic ordering. On the contrary, we can suspect a much stronger link between magnetism and the  $a$ -axis anomaly, which occurs at  $T_{min} \approx J_1 + J_2$  (Ref. 14). Unfortunately, the effect of this anomaly on the internal parameters is too small to be observed. Nevertheless, we can speculate that the main effect of this anomaly is to further *increase* the  $J_1/J_2$  ratio, pushing the system further towards the unfrustrated limit. It is noteworthy that the NNN interactions are uniformly violated in the simple Néel state. The spin Jahn-Teller mechanism requires exact cancelation between symmetry equivalent interactions of opposite sign, and is therefore not relevant here. Instead, the energy can be lowered simply by reducing the NNN in-

teraction. Unlike the case of  $Li_2VOSiO_4$ , this can occur *without* symmetry reduction, and should be observed well above  $T_N$  due to short-range magnetic correlations.

Our main conclusion is that  $VOMoO_4$  orders in a simple AFM Néel state, indicating a large  $J_1/J_2$  ratio. The V moment is significantly reduced from the spin-only value, consistent with a strongly 2D character and enhanced quantum fluctuations. Far from being a replica of  $Li_2VOSiO_4$ ,  $VOMoO_4$  must be assigned to a completely different part of the  $J_1/J_2$  phase diagram, and will provide independent verification of the theoretical models. Nevertheless, our measurements agree in many other respects with results obtained with local probes. In particular, our observation of structural anomalies above  $T_N$  confirms the possibility that the onset of magnetic order is coupled to the lattice.

Fruitful discussions with P. Carretta and R. Caciuffo are acknowledged.

- 
- <sup>1</sup>P. Chandra, P. Coleman, and A. I. Larkin, *Phys. Rev. Lett.* **64**, 88 (1990).
- <sup>2</sup>L. Capriotti, A. Fubini, T. Roscilde, and V. Tognetti, *Phys. Rev. Lett.* **92**, 157202 (2004).
- <sup>3</sup>J. Villain, R. Bidaux, J. P. Carton, and R. Conte, *J. Phys. (Paris)* **41**, 1263 (1980).
- <sup>4</sup>C. D. Batista and S. A. Trugman, *Phys. Rev. Lett.* **93**, 217202 (2004).
- <sup>5</sup>P. Millet and C. Satto, *Mater. Res. Bull.* **33**, 1339 (1998).
- <sup>6</sup>R. Melzi, P. Carretta, A. Lascialfari, M. Mambri, M. Troyer, P. Millet, and F. Mila, *Phys. Rev. Lett.* **85**, 1318 (2000).
- <sup>7</sup>R. Melzi, S. Aldrovandi, F. Tedoldi, P. Carretta, P. Millet, and F. Mila, *Phys. Rev. B* **64**, 024409 (2001).
- <sup>8</sup>A. Bombardi, J. Rodríguez-Carvajal, S. Di Matteo, F. de Bergevin, L. Paolasini, P. Carretta, P. Millet, and R. Caciuffo, *Phys. Rev. Lett.* **93**, 027202 (2004).
- <sup>9</sup>H. Rosner, R. R. P. Singh, W. H. Zheng, J. Oitmaa, S. L. Drechsler, and W. E. Pickett, *Phys. Rev. Lett.* **88**, 186405 (2002).
- <sup>10</sup>H. A. Eick and L. Kihlborg, *Acta Chem. Scand. (1947-1973)* **20**, 722 (1966).
- <sup>11</sup>I. Shiozaki, *J. Phys.: Condens. Matter* **10**, 9813 (1998).
- <sup>12</sup>I. Shiozaki, M. Ohashi, M. Koyano, and S. Katayama, *Physica B* **284–288**, 1621 (2000).
- <sup>13</sup>I. Shiozaki, *J. Magn. Magn. Mater.* **177–181**, 261 (1998).
- <sup>14</sup>P. Carretta, N. Papinutto, C. B. Azzoni, M. C. Mozzati, E. Pavarini, S. Gonthier, and P. Millet, *Phys. Rev. B* **66**, 094420 (2002).
- <sup>15</sup>F. Becca and F. Mila, *Phys. Rev. Lett.* **89**, 037204 (2002).
- <sup>16</sup>H. M. Rietveld, *J. Appl. Crystallogr.* **2**, 65 (1969).
- <sup>17</sup>J. Rodríguez-Carvajal, *Physica B* **55**, 65 (1993).
- <sup>18</sup>J. Rodríguez-Carvajal, *BASIREPS: A program for calculating irreducible representations of space groups and basis functions for axial and polar vector properties.* (See <ftp://ftp.cea.fr/pub/llb/divers/BasIreps>)
- <sup>19</sup>V. O. Kovalev, *Irreducible Representations of the Space Groups* (Gordon and Breach, New York, 1965).
- <sup>20</sup>Yu. A. Izyumov, *Neutron Diffraction of Magnetic Materials* (Consultants Bureau, New York, 1991).
- <sup>21</sup>H. J. Schulz, T. A. L. Ziman, and D. Poilblanc, *J. Phys. I* **6**, 675 (1996).
- <sup>22</sup>L. Siurakshina, D. Ihle, and R. Hayn, *Phys. Rev. B* **64**, 104406 (2001).